British Journal of Applied Science & Technology
4(19): 2821-2836, 2014

SCIENCEDOMAIN *international*
www.sciencedomain.org

Contributions on Closed System Transformations Based Thermal Cycles

Ramon Ferreiro Garcia[1*], Beatriz Ferreiro Sanz[1] and Cristina Ferreiro Sanz[1]

[1]Industrial Engineering Department, ETSNM, C/Paseo de Ronda 51, 15011, University of A Coruna, Spain.

Authors' contributions

This work was carried out in collaboration between all authors. Author RFG designed the study, wrote the protocol, the first draft of the manuscript and managed literature searches. Authors BFS and CFS managed the analyses of the study and literature searches. All authors read and approved the final manuscript.

Original Research Article

Received 14th March 2014
Accepted 29th April 2014
Published 21st May 2014

ABSTRACT

The research work is focused on novel feasible structures of non condensing mode trilateral thermal cycles which differs from the recently known trilateral thermal cycles in that the conversion of heat to mechanical work is performed undergoing closed process transformations along with the three state point changes of the cycle. The proposed cycle is characterised by the fact that in its active process, as heat energy is being absorbed under increasing specific volume, entropy and temperature undergoing a load-dependent path function, mechanical work is simultaneously performed, contrary to what happens in conventional Carnot based engines. An analysis of the proposed cycle is carried out and results compared with that of a Carnot cycle operating under the same ratio of temperatures. Into the range of relative low operating temperatures (320 K) high thermal efficiency is achieved reaching 25.4% for hydrogen, 36.3% for helium and 31.8% for argon as working fluids when compared with Carnot Factor (7.8%).

Keywords: Carnot factor; isobaric expansion; load-dependent path functions; thermal efficiency; trilateral cycle.

**Corresponding author: E-mail: ferreiro@udc.es;*

NOMENCLATURE

γ	adiabatic expansion coefficient
η	thermal efficiency (non regenerative cycle)
η_{23}	thermal efficiency of process (2)-(3)
Cp	specific heat capacity at constant pressure (kJ/kg-K)
Cv	specific heat capacity at constant volume(kJ/kg-K)
h	specific enthalpy (kJ/kg)
p	pressure (bar)
$q_i=q_{23}$	total specific input heat (kJ/kg)
$q_o=q_{21}$	specific rejected heat (kJ/kg)
s	specific entropy (kJ/kg-K)
T	temperature (K)
W_{23}	output specific work (kJ/kg)
W_N	net specific work (kJ/kg)
C_R	conversion ratio (W_{23}/q_{23})
T_R	Ratio of top to bottom temp. (T_3/T_1)

ABBREVIATIONS

CF	Carnot Efficiency
ORC	Organic Rankine Cycle
OTEC	Ocean Thermal Energy Convertor
NORC	Non Organic Rankine Cycle
TTC	Trilateral Thermal Cycle

1. INTRODUCTION

All the known thermal cycles under use so far are derived from the Carnot engine, which means quadrilateral cycles in which ideally heat is absorbed at constant temperature (top temperature) and work is delivered when temperature decreases from the top temperature to approach the bottom temperature under a quasi entropic transformation. The power cycles that obey to this model are classified in two main groups based on the nature of the working fluid: gas power cycles and vapour power cycle. The difference between the two groups is that in the first case the working fluid is gaseous and does not experiment any phase change, while for the second group, there is a liquid-vapour phase change process of the working fluid within the cycle. In Fig. 1 a simple classification of heat engines based cycles is depicted.

Some studies regarding trilateral thermal cycles have recently appeared in scientific literature. Thus, for instance, a comparison of trilateral cycles and organic Rankine cycles has been carried out by [1] in which a clear contribution to the thermal efficiency enhancement has been reported. Nevertheless, in the proposed present work, a different perspective of trilateral thermal cycle is being considered which is depicted in the Fig. 1. (the isobaric expansion based trilateral thermal cycle under not condensing mode, which also can be regenerative or non regenerative cycle, being based on a completely different thermal cycle concept in comparison with the conventional Carnot based thermal cycles, structurally but also in terms of Carnot factor (CF) constraints.

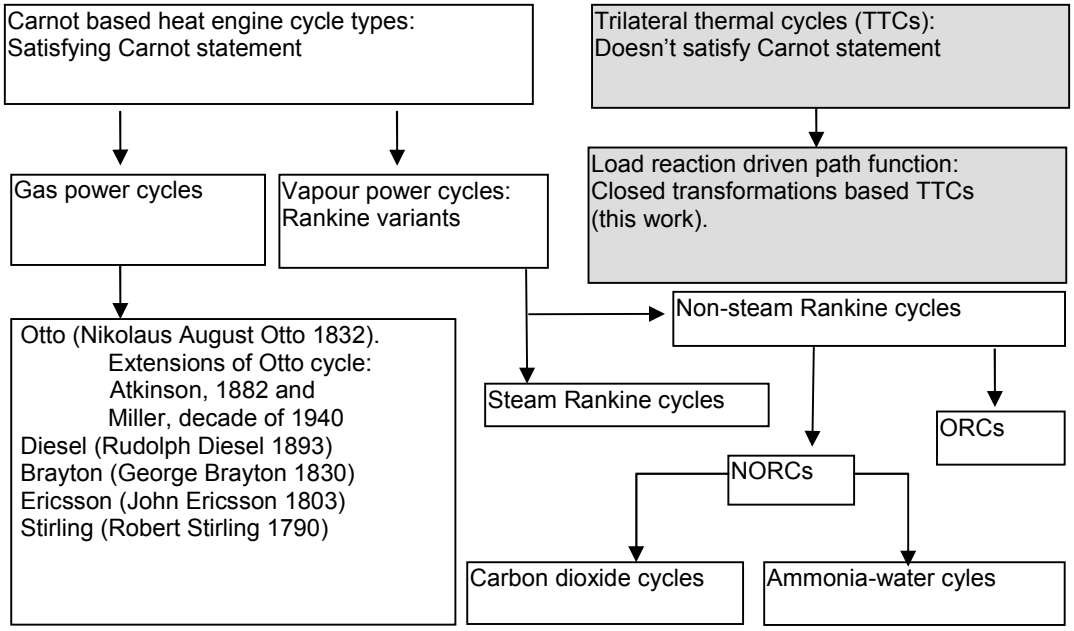

Fig. 1. Classification of Carnot and non Carnot based thermal engines: quadrilateral and trilateral thermal cycles

The objective of the study is to efficiently convert low temperature heat mainly from ocean thermal and solar thermal sources to be converted by means of the proposed thermal cycle and plant structure into electric energy. The proposed conversion method is based on a different thermodynamic cycle: the non condensing mode trilateral thermal cycle with or without regeneration. The proposed cycle is not based on the quadrilateral Carnot cycle but on the trilateral cycle which absorbs heat and performs mechanical work simultaneously between the states (2) and (3) of the trilateral cycle. As a consequence of this contribution, this cycle is not restricted by the CF constraints. Its maximum thermal efficiency is influenced not only by the ratio of the top to bottom temperatures like for instance in the cycles' analysis described in [2,3], but also by some factors such as the characteristics of the working fluids and regeneration capabilities when regeneration is considered.

In the low temperature range, bottoming ORCs constitute another alternative, having shown good thermodynamic performance for low maximum temperature bottoming cycles [4-6]. The interest in organic working fluids for residual heat applications with low temperature Rankine cycles is an old technique that has been proposed for different applications: renewable energy and low temperature heat recovery [4-15]. Furthermore, small scale ORC power plants are presently commercially available [12].

The work has been organised into 5 main sections, where section 2 is devoted to the description of the new thermodynamic concepts regarding the TTC included in the proposed contribution, section 3 describes the architecture of feasible OTEC or Solar plant configurations supporting the TTC, in section 4 a case study is included in which the performance analysis and discussion of results have been carried out on a feasible structure of the projected plant, and finally in section 5 some relevant conclusions are highlighted.

2. ANALYSIS OF THE HEATING PROCESS FOLLOWING LOAD-DEPENDENT PATH FUNCTIONS

In what follows, the studied trilateral thermal cycle undergoes three closed transformations instead of three open processes. Let's assume that heat is added to a unit mass of working fluid following an isobaric path function from the state point (2) to the state point (3) as shown in Fig. 2, undergoing a structure similar to that described in [4], and suppose the resulting expansion causes the total volume and the specific volume to increase from V_2 to V_3., the temperature from T_2 to T_3 and the entropy from s_2 to s_3.

The first principle for closed transformations where irreversibilities, potential and kinetic energy are neglected yields

$$\sum q - \sum W - \Delta u = 0 \rightarrow q_{23} - W_{23} = \Delta u = u_3 - u_2 \tag{1}$$

where the work W_{23} done by a unit mass of the working fluid is defined as

$$W_{23} = \int_{V2}^{V3} pdV = p_2(V_3 - V_2) = p_3(V_3 - V_2) \tag{2}$$

Equation (2) can be expressed according to the definition given in (1) yielding

$$W_{23} = q_{23} - \Delta u_{23} \tag{3}$$

The C_R (conversion ratio) or efficiency of this closed reversible transformation (2)-(3) is

$$C_R = \eta_{23} = \frac{W_{23}}{q_{23}} = \frac{q_{23} - \Delta u_{23}}{q_{23}} = 1 - \frac{\Delta u_{23}}{q_{23}} = 1 - \frac{Cv \cdot (T_3 - T_2)}{Cp \cdot (T_3 - T_2)} = 1 - \frac{1}{\gamma} \tag{4}$$

Surprisingly, the expression defining the C_R or transformation efficiency exhibits very low dependence on the temperature, that is, practically is not temperature dependent.

This suggests to us that for low top temperatures the Carnot efficiency is lower than the value of this ideal thermal efficiency, since when the top temperature approaches the bottom temperature CF tends towards zero.

Considering an approach to ideal gases such as helium or argon, the corresponding conversion ratio definition according to the data achieved from [16] yields

$$\eta_{23} = \frac{W_{23}}{q_{23}} = 1 - \frac{1}{\gamma_{He}} = 1 - \frac{1}{1.665} = 0.4 \quad \text{for helium as working fluid,} \tag{5}$$

$$\eta_{23} = 1 - \frac{1}{\gamma_{Ar}} = 1 - \frac{1}{1.67} = 0.4012 \quad \text{for argon, and,} \tag{6}$$

$$\eta_{23} = 1 - \frac{1}{\gamma_{H2}} = 1 - \frac{1}{1.41} = 0.29 \text{ for hydrogen} \quad (7)$$

for any temperature $T_3 > T_1$.

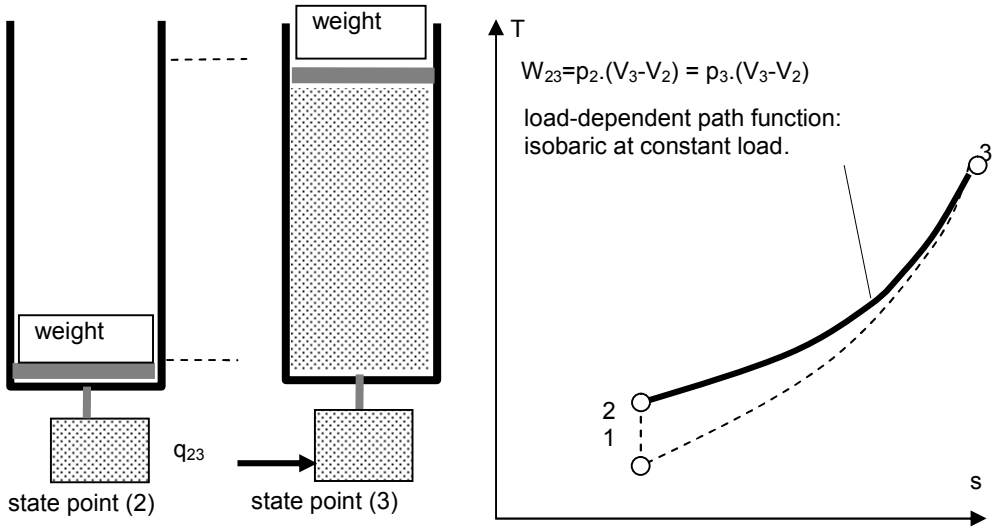

Fig. 2. The process of heating a working fluid at constant pressure (closed process). The fluid is confined into the heater and the cylinder. At constant load, the pressure is constant so that the heating process undergoes an isobaric path function

Nevertheless, in order to convert heat to mechanical work under useful modes, a thermal cycle must be applied, and this requirement undergoes the implementation of a thermal engine structure. In such case, the cycle efficiency η will not match the C_R for which the maximum efficiency could not be equal to the efficiency achieved in (4), so that $\eta < C_R$ to fulfil the 2^d law. Thus, next sub-section deals with such subject.

2.1 Analysis of a Trilateral Thermal Cycle Composed by Closed System Based Transformations

Considering now a thermal cycle composed by closed system based transformations, with reference to the Fig. 3 for the structure and Fig. 4 for the T-s and the p-V diagrams, follows that the energy balance of the TTC has been considered assuming that the process (2)-(3) is a closed transformation, since there is not exchange of matter, so that the amount of specific energy added from an external heat source is defined as

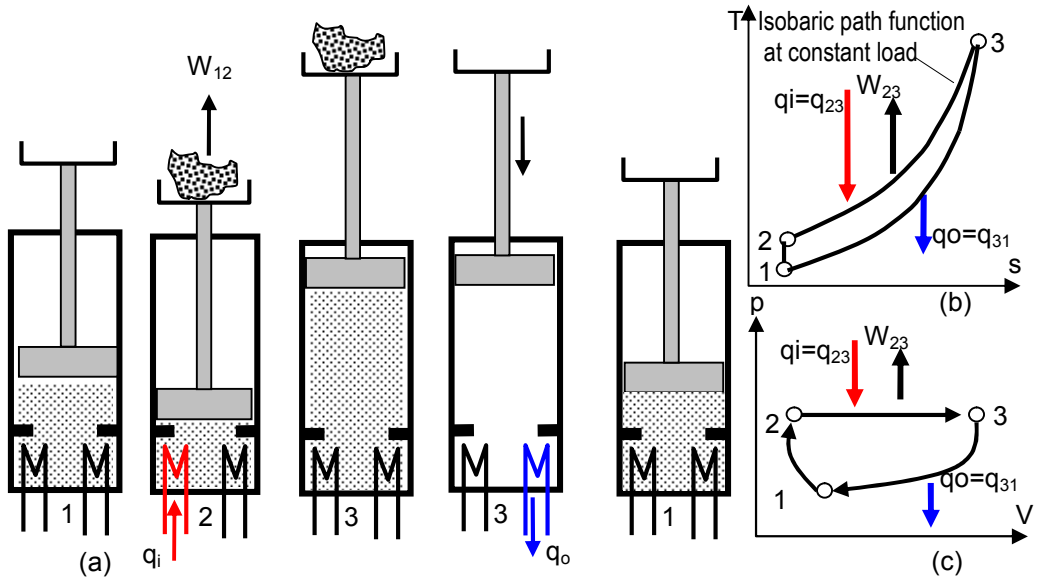

Fig. 3. A thermal cycle composed by closed systems transformations. (a), a trilateral cycle consisting of a cylinder that absorbs heat q_i, delivering work simultaneously along the transformation (2)-(3) and rejecting heat during the transformation (3)-(1). (b), the T-s diagram of the trilateral cycle. (c), the corresponding p-V diagram. At constant load, the pressure is constant so that the heating process undergoes an isobaric path function

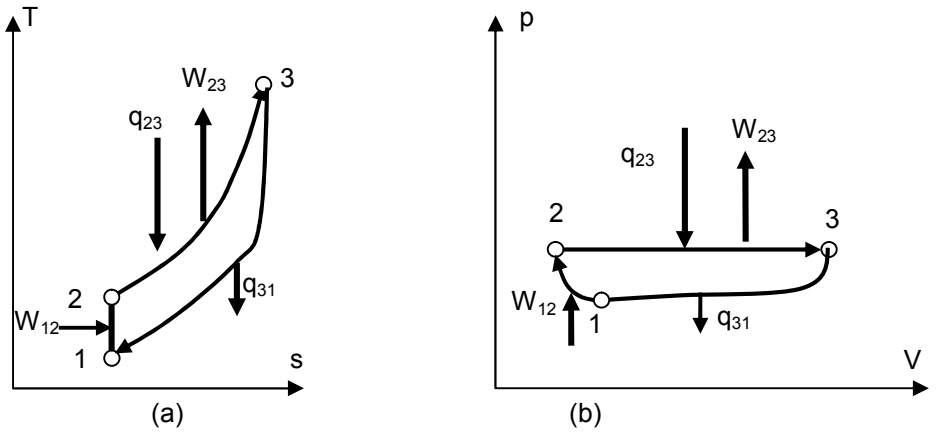

Fig. 4. Diagrams of the cycle. (a), T-s diagram. (b), p-V diagram

$$q_i = q_{23} = W_{23} + \Delta u_{23} = p_2 \cdot (V_3 - V_2) + u_3 - u_2 \tag{8}$$

and for the process (3)-(1) the amount of heat rejected to the low temperature heat sink considered also as a closed transformation yields

$$q_o = q_{31} = W_{31} + \Delta u_{31} = 0 + \Delta u_{31} = u_3 - u_1 \tag{9}$$

Consequently the net mechanical work is

$$W_N = q_i - q_o = q_{23} - q_{31} = W_{23} + \Delta u_{23} - \Delta u_{31} = W_{23} - u_2 + u_1 \tag{10}$$

Thus the thermal efficiency is given as

$$\eta = \frac{W_N}{q_i} = \frac{q_i - q_o}{q_i} = \frac{W_{23} + u_1 - u_2}{W_{23} + u_3 - u_2} \tag{11}$$

From (11) follows that the thermal efficiency can also be expressed in terms of the state point temperatures, so that

$$\eta = \frac{W_N}{q_{23}} = \frac{q_{23} - q_{31}}{q_{23}} = \frac{Cp \cdot (T_3 - T_2) - Cv \cdot (T_3 - T_1)}{Cp \cdot (T_3 - T_2)} = \\ = 1 - \frac{Cv \cdot (T_3 - T_1)}{Cp \cdot (T_3 - T_2)} = 1 - \frac{1}{\gamma} \frac{(T_3 - T_1)}{(T_3 - T_2)} \tag{12}$$

The maximum attainable ideal efficiency will be achieved as temperature T_2 approaches T_1, as shown below, yielding

$$\lim_{T_2 \to T_1} \eta = \lim_{T_2 \to T_1} 1 - \frac{1}{\gamma} \frac{(T_3 - T_1)}{(T_3 - T_2)} \to 1 - \frac{1}{\gamma} \tag{13}$$

The result given in (13) is similar to the result achieved by (4) which defines the maximum achievable efficiency. As can be observed, the maximum thermal efficiency is not dependent on any cycle temperature, but on the adiabatic expansion coefficient, so that this efficiency cannot be compared with the Carnot factor. Furthermore, as shown bellow, there are a range and ratio of operating temperatures for which a flagrant violation of Carnot statement without violating the Clausius or Kelvin statements (second law) exist. Furthermore, for low temperatures, the value corresponding to the expression (13) is greater than its corresponding CF. Consequently, Carnot statement is not applicable to load driven trilateral thermal cycles composed by closed systems based transformations.

Thus, since the ideal (maximum obtainable efficiency) is $\eta = 1 - \frac{1}{\gamma}$ and $CF = 1 - \frac{1}{T_R}$, follows

$$\text{that for } \eta = CF, \quad \gamma = T_R \tag{14}$$

which implies that

$$CF < \eta \quad \text{for } T_R < \gamma \tag{15}$$

Based on equation (14), the following statement is proposed:

"In the thermal cycles composed by closed system based transformations in which $T_3 > T_1$, there is a ratio of temperatures $T_R = T_3/T_1$ such that $\eta > CF$",

since for $T_R = 1$, (that is $T_3 = T_1$), CF = 0.

Thus, the maximum temperature T_3 for which $CF < \eta$ is achieved from (14) as

$$\gamma = T_R = \frac{T_3}{T_1}$$, resulting in

$$T_3 = T_1 \cdot \gamma \tag{16}$$

Assuming helium, argon and hydrogen as working fluids, and applying (16) to obtain the maximum temperatures for which the Carnot factor is lower than the thermal efficiency, the performed analysis yields the results shown in Table 1.

Table 1. The maximum temperature T_3 for which CF is lower than γ (adiabatic expansion coefficient) for helium, argon and hydrogen as working fluids

	γ	T_1(K)	T_3 (K)
He	1.665	295	491.2
Ar	1.67	295	492.6
H_2	1.41	295	416

3. A CASE STUDY BASED ON THE THERMAL CYCLE COMPOSED BY CLOSED SYSTEMS BASED TRANSFORMATIONS

Two different and optional engine structures to implement a trilateral thermal cycle composed by closed system based transformations are depicted with Fig 5 and Fig 6 respectively. In Fig. 5 it is implemented a trilateral thermal cycle by means of a pair of bellows type actuators operating optionally with helium, hydrogen, or argon, as well as other gases, which is equipped with heating and cooling facilities: This bellows type actuators acts a pneumatic piston used to drive a reciprocating hydraulic pump which drives a turbine by means of a hydraulic circuit. Although not analysed in this work and consequently not represented in Fig. 5, the possibility of regenerating some residual heat between both bellows type cylinders exits. Since this is not the objective of the research, the possibility of increasing a bit the thermal efficiency is a real fact. The thermal cycle depicted in Fig 5 can be completed by means of performing the next semi-cycle interchanging the role of each bellows-type actuator. Summarising, the role of each bellows is reversed every semi-cycle.

The functioning of the plant depicted in Fig. 5 is as follows: Assuming the chamber 1 active, the heating port X is open to heat the working fluid confined into the chamber 1 under a closed system transformation approaching the pressure p_2 at constant load, and simultaneously mechanical work is being delivered. The conditions specified by the upper table depicted in Fig. 5 are met. Simultaneously, chamber 2 is being cooled through the port W to keep the pressure near p_1. During the next semi-cycle the role of each bellows type cylinder is changed in order to fulfill the conditions specified by the lower table depicted in Fig. 5, completing the cycle.

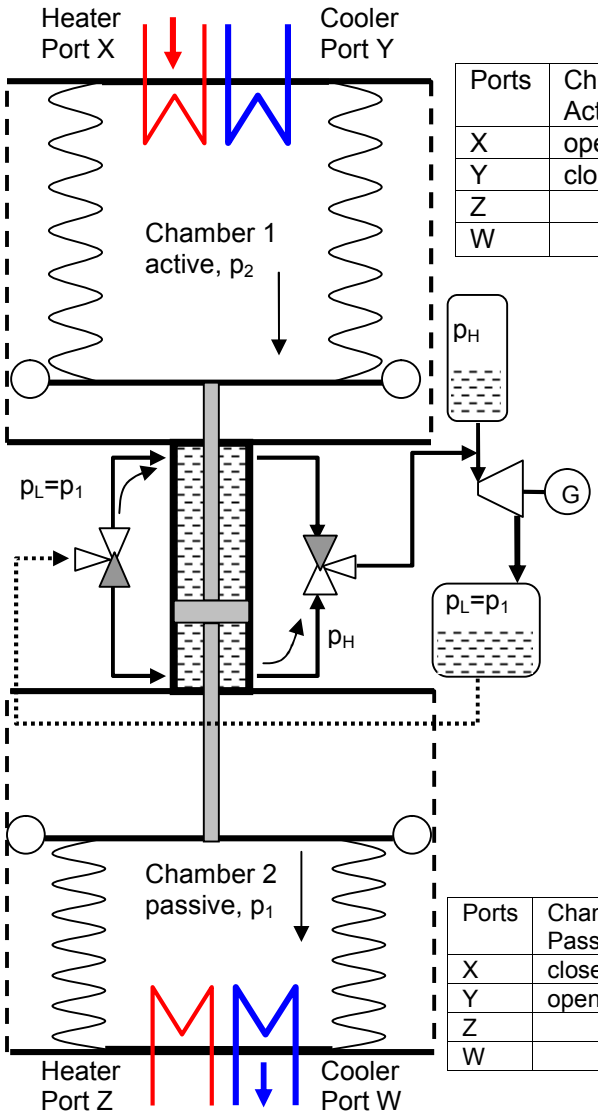

Ports	Chamber 1 Active, $p=p_2$	Chamber 2 Passive, $p=p_1$
X	open	
Y	closed	
Z		closed
W		open

Ports	Chamber 1 Passive, $p=p_1$	Chamber 2 Active, $p=p_2$
X	closed	
Y	open	
Z		open
W		closed

Fig. 5. A closed cycle implemented under a pair of bellows type actuators operating optionally with helium, hydrogen, or argon as working fluids, and with the same fluid into both chambers. The status corresponds to the chamber 1 active with ($p=p_2$) and chamber 2 passive with ($p=p_1$)

As above mentioned, the described trilateral thermal cycle could be implemented under different optional mechanical structures; therefore, in Fig. 6 a scheme based on a pair of thermo-hydraulic cylinders equipped with heating and cooling devices is depicted. Since the efficiency is relatively high at low temperatures, which can approach a range of values between (29%-36%) according to the results shown in Table 4, the appropriate temperatures can be achieved by direct solar radiation to operate between 295 and 320 K.

The thermo-hydraulic cylinder contains the same amount of gas at the top side (thermal working fluid) and the corresponding amount of hydraulic fluid in the bottom side whose oil level depends on the thermo-hydraulic operating status. The heated working fluid (gas) pushes the hydraulic fluid through the hydraulic circuit to drive a hydraulic turbine. As in the previous case depicted in Fig. 5, the role of each cylinder and valves in Fig. 6 is reversed every semi-cycle.

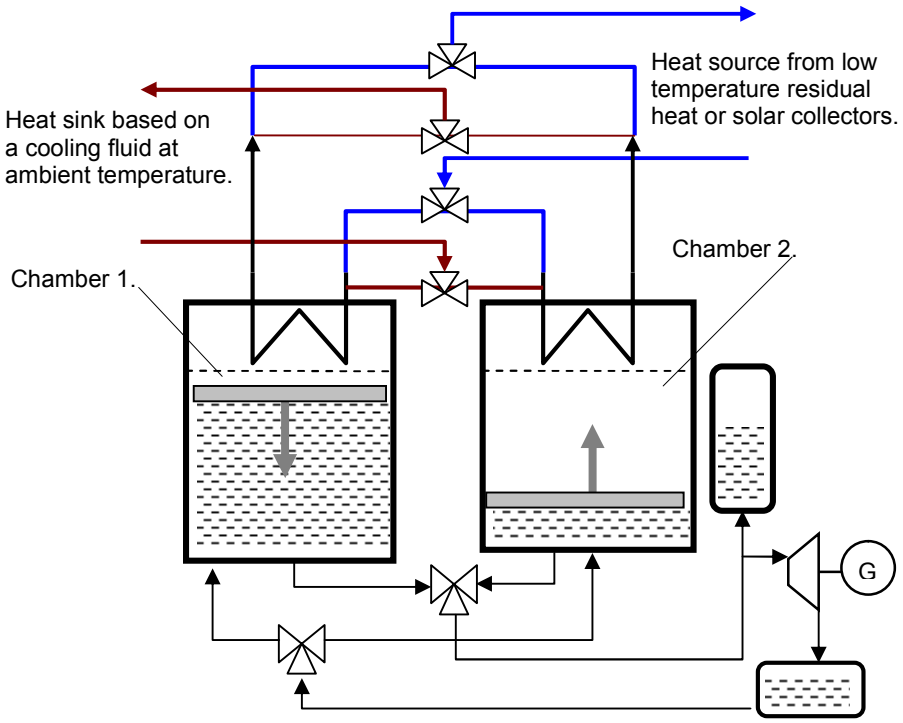

Fig. 6. An optional structure of the trilateral thermal cycle composed of closed process based transformations, composed of a pair of thermo-hydraulic cylinders equipped with heating and cooling devices

The plant structure depicted in Fig. 6 is composed of two hydraulic piston type thermo-hydraulic cylinders, which exhibit the ability to convert thermal energy to hydraulic power by pushing down a hydraulic fluid that drives a hydraulic turbine. The functioning of the plant depicted in Fig. 6 is as follows: Assuming the chamber 1 active (left thermo-hydraulic cylinder), the corresponding heating port is open to heat the working fluid confined into the chamber 1 under a closed system transformation approaching the pressure p2 at constant load, and simultaneously mechanical work is being delivered by pushing the hydraulic piston down to drive a hydraulic turbine. Simultaneously, chamber 2 is being cooled through the corresponding port to keep the pressure near p1, favouring the returning of the hydraulic fluid into the chamber 2. During the next semi-cycle the role of each hydraulic cylinder is changed in order to perform the next semi-cycle, thus completing the trilateral cycle.

Although not represented in the plant structures chosen for the case study, the two existing modes of regeneration such as a thermal fluid mixing based regeneration, or a heat transfer based regeneration, could be also implemented which will contribute to the efficiency

enhancement as a continuation to this work. However this topic is out off the scope of this work.

4. A CASE STUDY: ANALYSIS AND DISCUSSION

In this section the proposed case study with results concerning to the non condensing mode trilateral thermal cycle in which the conversion of heat to mechanical work is performed undergoing closed process transformations, operating optionally with helium, argon or hydrogen is described. The data used in the case study is extracted from [16]. Thus in Table A1 of the appendix A the correspondent data of the TTC operating with He, Ar and H_2 as working fluid is presented. A range of low temperatures between 305 and 320 K are studied. However the temperature of the heat power supply (preferably thermal solar heat) will be at least 10 degrees higher than the top temperature T_3 of the cycle.

Based on the data of Table A1, the thermal efficiency of the TTC has been computed for several maximum temperatures of the TTC. The results are shown in Table 2. According to the achieved results, within the range of maximum temperatures between 305 and 320 K, the thermal efficiency is higher than the CF for all considered working fluids. The Table 2 shows the thermal efficiency, Carnot factor and the specific work for the considered working fluids. As shown in Table 2, although γ (the adiabatic expansion coefficient) for argon is greater than for the helium and hydrogen, the specific work is too much lower, which will require a considerable mass flow rate as well as a different plant structure in terms of size and weight to permit such mass flow rate. Consequently, argon could be discarded if helium is available. However as shown in Table 2, the specific work for hydrogen as working fluid, is significantly greater than that of the helium, which requires a smaller volumetric size than for helium. On the other hand the efficiency is lower. According to these considerations perhaps the best option is helium because of its associated characteristics such as stability, price, and availability.

4.1 The Influence of the Working Pressure on the Efficiency and Specific Work

In this subsection an analysis of the proposed case study is in which a wide range of operating pressures (4-400 bar) under the same temperatures (305-320 K) for helium as working fluid is considered. The cycle's data is shown in Table A2, and the corresponding results are shown in Table 3.

According to the results shown in Table 3 both the thermal efficiency and specific work increase slightly as pressure decreases. This phenomenon is advantageous because the lower working pressure, more simple is the plant from the structural point of view. However, specific volume (as shown in the righter column of Table A2) increases dramatically associated to the decreasing of pressure, which leads to an exaggerated plant size with its associated weight. Therefore there must be a compromise between the two concepts.

However the power plant investigated in [17] will be taken as reference to compare performance results. Thus, in [17] it is reported a thermal efficiency of η[17] = 1.9% at a top temperature of 299 K, while the overall efficiency approaches η_N[17]= 1.2 %. This means that the overall losses due to internal and external irreversibilities in the plant described in [17] approaches a net efficiency (η_N) given as η_N[17]/η[17]= (1.2/1.9)= 0.63.

Table 2. The thermal efficiency, Carnot factor and the specific work for the considered working fluids

T_3(K)	305	310	315	320
CF(%)	3.28	4.84	6.35	7.81
He				
η(%)	28.88	32.79	36.7	36.63
W(kJ/kg)	12.81	23.05	36.49	43.49
Ar				
η(%)	29.11	30.52	31.28	31.79
W(kJ/kg)	2.11	3.45	4.79	6.13
H_2				
η(%)	20.35	23.25	24.61	25.39
W(kJ/kg)	27.08	48.28	69.44	90.56

Table 3. The thermal efficiency, Carnot factor and the specific work for helium as working fluids under maximum operating pressures of 400, 40 and 4 bar

T_3(K)	305	310	315	320
CF(%)	3.28	4.84	6.35	7.81
p_2=p_3=400 bar				
η(%)	28.88	32.79	36.7	36.63
W(kJ/kg)	12.81	23.05	36.49	43.49
p_2=p_3=40 bar				
η(%)	29.3	33.23	35.04	36.09
W(kJ/kg)	12.93	23.29	33.65	44.01
p_2=p_3=4 bar				
η(%)	29.54	33.42	35.18	36.22
W(kJ/kg)	13.07	23.47	33.83	44.23

Consequently, the net efficiency for the proposed TTC can be approached as

$$\eta_N = \frac{\eta_N[17]}{\eta[17]} \cdot \eta \tag{17}$$

Assuming the losses for the proposed TTC similar to the losses of the experimented in [17], because of its structural similarities with respect to its heat exchangers, the overall efficiency for the proposed TTC can be estimated as

$$\eta_N = \frac{\eta_N[17]}{\eta[17]} \cdot \eta = \frac{1.2}{1.9} \cdot \eta = 0.63 \cdot \eta \tag{18}$$

Table 4. Estimated net efficiency for the TTC as function of the top operating temperatures using information from the reference [16]

T_3(K)	305	310	315	320
CF (%)	3.28	4.84	6.35	7.81
η_{He} (%)	18.61	21.05	22.16	22.81
η_{Ar} (%)	18.34	19.23	19.71	20.03
η_{H2} (%)	12.8	14.65	15.50	16.00

Therefore, the net TTC thermal efficiency has been computed for the same top temperatures assumed for the case study shown in Table 2. As noted from Table 4, net efficiencies are the 63% of the theoretical thermal efficiency, yet substantially higher than both, the Carnot factor and the engine studied in [9].

5. CONCLUSION

The study on closed systems based trilateral thermal cycles which differs from the trilateral thermal cycles composed of open systems based transformations, in that the conversion of heat to mechanical work is performed undergoing closed systems transformations along with the three state point changes of the cycle has been presented. As shown along the work, also differs from the quadrilateral Carnot based cycles in that the thermal working fluid absorbs heat from a heat source (low temperature thermal solar collector) and simultaneously, undergoing a load based pressure path function (isobaric process for constant loads), converts a fraction of this heat into mechanical work. The proposed TTC has been studied for helium, argon and hydrogen as thermal working fluids; although any other gas with good characteristics (high adiabatic expansion coefficient) will be useful since efficiency is a function of the adiabatic expansion coefficient. According to the characteristics of the proposed TTC, new expressions for the thermal efficiency have been achieved and analysed.

The performance results of the TTC have been compared with the results obtained for the Carnot cycle, both operating between the same range and ratio of temperatures.

An important conclusion is related to:

- The TTC structure which is configured under three closed system based transformations and,
- The thermal efficiency of the cycle which exceeds the Carnot efficiency under appropriated operating conditions. Furthermore, the maximum thermal efficiency is a linear function of the adiabatic expansion coefficient.
- Since the efficiency is not a function of the top temperature, the plant can operate at a very low temperature even rendering an efficiency approaching the value of the adiabatic expansion coefficient.

The reason obeys to the fact that in a trilateral cycle, isobaric heat absorption and simultaneous conversion into mechanical work and residual heat, take place simultaneously during a cycle transformation. Furthermore, thermal losses due to isentropic efficiency are avoided if reversible transformations can be approached.

The most important conclusion is related to the high net thermal efficiency, which in the best case has been estimated as 22.81% versus 7.81% for Carnot cycle as shown in Table 4.

As shown by the results, the ideal thermal efficiency is significantly increased in comparison with the actual conventional ORCs. An overall conclusion concerns to the fact that a new family of efficient power plants operating at low temperatures using oceanic thermal energy [17] as well as solar or residual heat is possible.

COMPETING INTERESTS

Authors have declared that no competing interests exist.

REFERENCES

1. Johann Fischer. Comparison of trilateral cycles and organic Rankine cycles. Energy. 2011;36:6208-6219. Available: http://dx.doi.10.1016/j.energy.2011.07.041
2. Kaushik SC, SivaRedd V, Tyagi SK. Energy and exergy analyses of thermal power plants: A review. Renewable and Sustainable Energy Reviews. 2011;15:1857-1872.
3. Jing Li, Gang Pei, Yunzhu Li, Dongyue Wang, Jie Ji. Energetic and exergetic investigation of an organic Rankine cycle at different heat source temperatures. Energy. 2012;38:85-95.
4. Yamamoto T, Furuhata T, Arai N, Mori K. Design and testing of the Organic Rankine Cycle. Energy. 2001;26:239-251.
5. Angelino G, Colonna P. Multicomponent working fluids for Organic Rankine Cycles (ORC). Energy. 1998;23(6):449-463.
6. Prabhu E. Solar trough Organic Rankine electricity system (STORES) stage 1: Power plant optimization and economics. Subcontract Report NREL/SR-550-39433; 2006.
7. Saleh B, Koglbauer G, Wendland M, Fischer J. Working fluids for low temperature Organic Rankine Cycles. Energy. 2006;32(7):1210-1221.
8. Hung T. Waste heat recovery of Organic Rankine Cycle using dry fluids. Energy Conversion and Management. 2001;42:539-553.
9. Borsukiewicz-Gozdur A, Nowak W. Comparative analysis of natural and synthetic refrigerants in application to low temperature Clausius–Rankine cycle. Energy. 2007;32(4):344-352.
10. Hung TC, Shai TY, Wang SK. A review of Organic Rankine Cycles (ORCs) for the recovery of low-grade waste heat. Energy. 1997;22(7):661-667.
11. Mago PJ, Chamra LM, Srinivasan K, Somayaji C. An examination of regenerative Organic Rankine Cycles using dry fluids. Applied Thermal Engineering. 2008;28:998-1007.
12. Joan Carles Bruno, Jesus Lopez-Villada, Eduardo Letelier, Silvia Romera, Alberto Coronas. Modelling and optimisation of solar Organic Rankine Cycle engines for reverse osmosis desalination. Applied Thermal Engineering. 2008;28:2212-2226. DOI: 10.1016/j.applthermaleng.2007.12.022.
13. Huijuan Chen, Yogi Goswami D, Elias K. Stefanakos. A review of thermodynamic cycles and working fluids for the conversion of low-grade heat. Renewable and Sustainable Energy Reviews. 2010;14:3059-3067.
14. Wei D, Lu X, Lu Z, Gu J. ji C. Performance analysis of different working fluids for use in Organic Rankine Cycles. Proc IM Performance analysis and optimization of Organic Rankine Cycle (ORC) for waste heat recovery. Energy Conversion and Management. 2007;48:1113-1119.
15. Drescher U, Brüggemann D. Fluid selection for the Organic Rankine Cycle (ORC) in biomass power and heat plants. Applied Thermal Engineering. 2007;27(1):223-228.
16. Lemmon EW, Huber ML, McLinden MO. NIST Reference Fluid Thermodynamic and Transport Properties - REFPROP Version 8.0, User's Guide, NIST 2007, Boulder, Colorado; 2010.
17. Semmari H, Stitou D, Mauran S. A novel Carnot-based cycle for ocean thermal energy conversion. Energy. 2012;43:361-375.

APPENDIX

A. The Data for the Case Study

Table A1. Data applied on the case study for the TTC operating with He, Ar and H_2 as working fluids using data from [17]

Point	T_3(K)	h(kJ/kg)	u(kJ/kg)	s(kJ/kg.K)	p(bar)	V(m^3/kg)
He						
1	295	1663	936.72	15.561	395	0.018387
2	296.4	1673.71	941.39	15.561	400	0.018267
3	320	1794.2	1015.3	15.957	400	0.019471
3	315	1768.3	999.66	15.876	400	0.019296
3	310	1742.4	983.96	15.793	400	0.018960
3	305	1716.4	968.27	15.709	400	0.018704
Ar						
1	295	104.13	39.074	2.4809	395	0.001647
2	296.2	105.11	39.324	2.4809	400	0.001641
3	320	124.25	52.228	2.5436	400	0.001801
3	315	120.28	49.601	2.5311	400	0.001767
3	310	116.27	46.931	2.5182	400	0.001734
3	305	112.21	44.215	2.5050	400	0.001700
H_2						
1	295	4112.8	2588.6	28.380	395	0.038587
2	296.1	4135.51	2599.4	28.380	400	0.038319
3	320	4488.8	2854.7	29.538	400	0.040853
3	315	4414.3	2801.3	29.304	400	0.040325
3	310	4339.8	2748.0	29.065	400	0.039796
3	305	4265.3	2694.6	28.823	400	0.039266

Table A2. Data applied on the case study for the TTC operating with He as working fluid at 400, 40 and 4 bar, using data from [17]

Point	T_3(K)	h(kJ/kg)	u(kJ/kg)	s(kJ/kg.K)	p(bar)	V(m^3/kg)
p_2=p_3= 400 bar						
1	295	1663	936.72	15.561	395	0.018387
2	296.4	1673.71	941.39	15.561	400	0.018267
3	320	1794.2	1015.3	15.957	400	0.019471
3	315	1768.3	999.66	15.876	400	0.019296
3	310	1742.4	983.96	15.793	400	0.018960
3	305	1716.4	968.27	15.709	400	0.018704
p_2=p_3= 40 bar						
1	295	1549.9	925.85	20.308	39.5	0.158000
2	296.5	1559.31	930.56	20.308	40	0.156830
3	320	1679.9	1003.8	20.704	40	0.169010
3	315	1653.9	988.23	20.622	40	0.166420
3	310	1628	972.64	20.539	40	0.163830
3	305	1602	957.05	20.455	40	0.161240
p_2=p_3= 4 bar						
1	295	1538.4	924.53	25.086	3.95	1.554200
2	296.48	1547.46	929.14	25.086	4	1.542500
3	320	1668.3	1002.4	25.482	4	1.664600
3	315	1642.3	986.86	25.401	4	1.638600
3	310	1616.4	971.28	25.318	4	1.612700
3	305	1590.4	955.7	25.233	4	1.586700

Peer-review history:
The peer review history for this paper can be accessed here:
http://www.sciencedomain.org/review-history.php?iid=522&id=5&aid=4635